Molecular Anchoring of Duplex and Triplex DNA by Disubstituted Anthracene-9,10-diones: Calorimetric, UV Melting, and Competition Dialysis Studies

Ihtshamul Haq,[†] John E. Ladbury,[‡] Babur Z. Chowdhry,[†] and Terence C. Jenkins*[,§]

Contribution from the School of Chemical and Life Sciences, The University of Greenwich, Wellington Street, London SE18 6PF, UK, Department of Biochemistry, University College London, Riding House Street, London W1P 8BT, UK, and CRC Biomolecular Structure Unit, The Institute of Cancer Research, Cotswold Road, Sutton, Surrey SM2 5NG, UK

Received June 6, 1996[⊗]

Abstract: Isothermal titration calorimetry, UV melting, and competition dialysis techniques have been used to examine the binding of isomeric 1,4- and 2,6-bis(ω-aminopropionamido)-substituted anthracene-9,10-diones (anthraquinones) with $dA_n{\cdot}dT_n$ duplexes and $dT_n-dA_n{\cdot}dT_n$ triplexes. Recent footprinting studies [Fox, K. R.; Polucci, P.; Jenkins, T. C.; Neidle, S. *Proc. Natl. Acad. Sci. U.S.A.* **1995**, *92*, 7887−7891] indicate that 2,6 derivatives, but *not* their 1,4 counterparts, differentially stabilize triple-stranded DNA and may have application in antigene chemotherapy. Thermodynamic investigations are here reported for interaction with $dA_{18}{\cdot}dT_{18}$ and $dT_{18}-dA_{18}{\cdot}dT_{18}$. The 2,6 compound shows preferential triplex binding, with K_b values of 1.8×10^4 M (duplex)$^{-1}$ and 2.2×10^5 M (triplex)$^{-1}$ at 25 °C in aqueous solution, pH 6.0, whereas the 1,4 isomer favors duplex binding, with K_b values of 1.1×10^5 M (duplex)$^{-1}$ and 3.5×10^4 M (triplex)$^{-1}$. Binding to the preferred DNA is *enthalpically driven* for each ligand, whereas binding to the disfavored DNA is either *entropically driven* or enthalpy/entropy compensated. Further, the binding site sizes (3.6 base pairs/base triplets) suggest DNA intercalation. Competition dialysis studies with poly(dA)·poly(dT) and poly(dA)·poly$(dT)_2$ confirm these binding preferences, and qualitative support is provided from UV melting experiments. Such studies reveal triplex disruption by the 1,4 isomer at low drug concentrations while the 2,6 compound effects stabilization toward thermal triplex denaturation. Spectrophotometric studies of each free ligand indicate self-association in aqueous solution, with dimerization constants at 25 °C of $(2.9 \pm 0.2) \times 10^3$ and $(3.2 \pm 0.1) \times 10^3$ M^{-1} respectively for the 1,4 and 2,6 isomers. Taken together, these data provide a firm thermodynamic basis for the contrasting duplex/triplex binding preferences of this isomeric family of ligands.

Introduction

The ability of DNA to form triple-helical structures has been known for almost 40 years.[1,2] Current interest in triplex DNA has largely been stimulated by potential applications of triplex-forming oligonucleotides (TFOs) as therapeutic agents, particularly as part of a DNA duplex-targeted antigene strategy.[3,4] Thus, for example, a TFO may be used to artificially control the expression of regulatory genes by inhibiting either transcription or regulatory protein binding after sequence-selective recognition and hybridization to a target double-stranded DNA site (for reviews, see refs 2−4). Several recent studies have highlighted the biological potential and viability of the oligonucleotide-directed antigene approach.[5,6]

Intermolecular DNA triplexes can form when an oligopyrimidine strand binds in the major groove of a host homopurine·homopyrimidine duplex sequence, with the formation of T−A·T and C^+−G·C (i.e., Py−Pu·Py) base triplets, such that the introduced strand adopts a parallel orientation relative to the host purine strand. In the latter case this only occurs at low pH (≤5.5) since the third-strand cytosines must be ring protonated to facilitate interstrand hydrogen bonding. An alternative triplex can be produced when an oligopurine strand binds to the DNA duplex in an antiparallel fashion, leading to A−T·A and G−C·G (i.e., Pu−Py·Pu) triplets.[2,7] Hence, subject to certain conditions,[4,8] site-specific triplex binding can lead to a recognition of target DNA duplex sequences.

Triplex instability under physiological conditions represents a major limiting difficulty to the therapeutic use of TFOs, since the C^+−G·C triplet requires a low pH and the T−A·T triplet is only stable under conditions of high ionic strength. Several

* Author to whom correspondence should be addressed at the following: The Institute of Cancer Research−telephone (+44) 181 643-8901, FAX (+44) 181 770-7893, E-mail t.jenkins@icr.ac.uk.

† University of Greenwich.

‡ University College London.

§ The Institute of Cancer Research.

⊗ Abstract published in *Advance ACS Abstracts,* October 1, 1996.

(1) Felsenfeld, G.; Davies, D. R.; Rich, A. *J. Am. Chem. Soc.* **1957**, *79*, 2023−2024.

(2) Soyfer, V. N.; Potaman, V. N. *Triple-Helical Nucleic Acids*; Springer-Verlag: New York, 1996.

(3) Hélène, C. *Anti-Cancer Drug Des.* **1991**, *6*, 569−584.

(4) Thuong, N. T.; Hélène, C. *Angew. Chem., Int. Ed. Engl.* **1993**, *32*, 666−690.

(5) (a) McShan, W. M.; Rossen, R. D.; Laughter, A. H.; Trial, J.; Kessler, D. J.; Zendegui, J. G.; Hogan, M. E.; Orsan, F. M. *J. Biol. Chem.* **1992**, *267*, 5712−5721. (b) Ing, N. H.; Beekman, J. M.; Kessler, D. J.; Murphy, M.; Jayaraman, K.; Zendegui, J. G.; Hogan, M. E.; O'Malley, B. W.; Tsai, M. J. *Nucleic Acids Res.* **1993**, *21*, 2789−2796. (c) Grigoriev, M.; Praseuth, D.; Guieysse, A. L.; Robin, P.; Thuong, N. T.; Hélène, C.; Harrel-Bellan, A. *Proc. Natl. Acad. Sci. U.S.A.* **1993**, *90*, 3501−3505.

(6) (a) Helm, C. W.; Shrestha, K.; Thomas, S.; Shingleton, H. M.; Miller, D. M. *Gynacol. Oncol.* **1993**, *49*, 339−343. (b) Mayfield, C.; Ebbinghaus, S.; Gee, J.; Jones, D.; Rodu, B.; Squibb, M.; Miller, D. *J. Biol. Chem.* **1994**, *269*, 18232−18238. (c) Vasquez, K. M.; Wensel, T. G.; Hogan, M. E.; Wilson, J. H. *Biochemistry* **1995**, *34*, 7243−7251. (d) Macaulay, V. M.; Bates, P. J.; McLean, M. J.; Rowlands, M. G.; Jenkins, T. C.; Ashworth, A.; Neidle, S. *FEBS Lett.* **1995**, *372*, 222−228.

(7) Howard, F. B.; Miles, H. T.; Ross, P. D. *Biochemistry* **1995**, *34*, 7135−7144.

(8) (a) Roberts, R. W.; Crothers, D. M. *Proc. Natl. Acad. Sci. U.S.A.* **1991**, *88*, 9397−9401. (b) Mergny, J-L.; Sun, J-S.; Rougeé, M.; Montenay-Garestier, T.; Barcelo, F.; Chomilier, J.; Hélène, C. *Biochemistry* **1991**, *30*, 9791−9798.

S0002-7863(96)01907-5 CCC: $12.00 © 1996 American Chemical Society

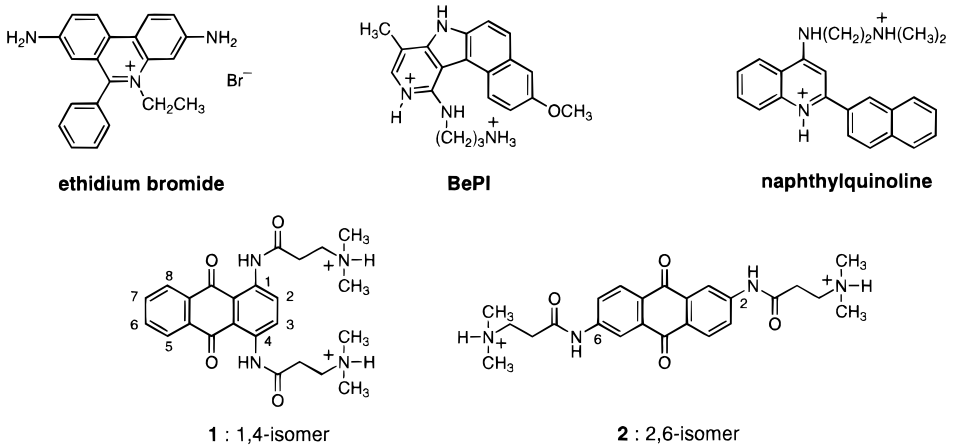

Figure 1. Structures of known DNA triplex-stabilizing intercalants together with the functionalized anthracene-9,10-diones examined in this study, showing the substituents at the 1,4 and the 2,6 ring positions for **1** and **2**, respectively.

approaches have been used to enhance either triplex stability or third-strand binding affinity.[2] Thus, for example, attachment of a DNA duplex-intercalating chromophore to the TFO can effectively "clamp" the third strand to the target by binding to duplex regions near the triplex−duplex junction.[4] Adaptations of this approach have also been used to effect covalent fixation of the third strand to the duplex through formation of photo-induced cross-links.[4,5c,6d,9]

One alternative strategy to improve triplex stability involves the use of adjuncts that show preferential binding to triple- rather than double-stranded DNA. To this end, both intercalator and groove-binding classes of ligand have been evaluated to assess possible triplex-specific binding properties.[2] However, the data accumulated for established duplex minor groove binders reveal generally poor stabilization of triplex DNA such that, for example, both netropsin[10] and distamycin[11] bind to triplex but destabilize it relative to the precursor duplex. In contrast, netropsin and other minor groove ligands (e.g., berenil and DAPI) can effectively stabilize mixed DNA−RNA triplexes.[12] Further, DNA triplex binding by berenil is remarkably sensitive to Na^+ concentration, with thermal stabilization of the triplex only at low or non-physiological [Na^+] levels.[13]

Numerous DNA intercalants have also been examined (Figure 1), including ethidium bromide,[14] coralyne,[15] benzo[*e*]pyrido-[4,3-*b*]indoles (e.g., BePI),[16] and a series of functionalized quinolines.[17] It is now established that large, crescent-shaped or extended planar molecules bearing a degree of rotational flexibility can provide strong DNA triplex stabilization,[2,17] particularly for triple helices that are rich in T−A·T triplets, as revealed by biophysical and spectroscopic techniques, including footprinting and hydrodynamic studies.

In a rational program to design analogues of the clinical antitumor agents adriamycin and mitoxantrone, both mono- and difunctionalized amidoanthracene-9,10-dione (anthraquinone) derivatives have been developed[18] (e.g., **1** and **2** in Figure 1). It has been shown that their DNA binding characteristics and biological response are profoundly influenced by the position of the substituent(s).[18,19] Thus, for example, kinetic studies and biophysical methods reveal that "simple" and 1,4-disubstituted compounds can bind to duplex DNA by a classical intercalation mode, whereas the binding of 2,6-disubstituted agents may involve a nonclassical intercalative "threading" process. In the latter case, the functionalized side chains are accommodated simultaneously within both the DNA minor and major groove conduits following intercalation of the planar chromophore. These binding mechanisms are supported by extensive molecular modeling.[18,20]

In a recent extension of these principles,[21] molecular modeling and DNA footprinting techniques have been used to show that symmetric 2,6-difunctionalized bis(propionamido)anthraquinones but *not* their 1,4 isomers can bind preferentially to triple-stranded DNA. These experimental results agree with modeling predictions of distinct intercalative binding modes, where threading of the ring substituents in the 2,6 derivatives through the stacked base planes leads to a selective triplex stabilization.[21] Based on these data we hypothesized that the structural basis underlying the DNA binding preferences of these ligands will be reflected in the thermodynamics of their DNA−ligand interactions.

In the present study we examine the duplex- and triplex-binding behaviors of two isomeric anthracene-9,10-dione ("anthraquinone") compounds of this family that differ solely in the ring positions used for attachment of pendant, protonatable

(9) (a) Duval-Valentin, G.; Thuong, N. T.; Hélène, C. *Proc. Natl. Acad. Sci. U.S.A.* **1992**, *89*, 504−508. (b) Havre, P. A.; Gunther, E. J.; Gasparro, F. P.; Glazer, P. M. *Proc. Natl. Acad. Sci. U.S.A.* **1993**, *90*, 7879−7883. (c) Gasparro, F. P.; Havre, P. A.; Olack, G. A.; Gunther, E. J.; Glazer, P. M. *Nucleic Acids Res.* **1994**, *22*, 2845−2852. (d) Deglos, G.; Clarenc, J. P.; Lebleu, B.; Lonetti, J. P. *J. Biol. Chem.* **1994**, *269*, 16933−16937.

(10) Park, Y-W.; Breslauer, K. J. *Proc. Natl. Acad. Sci. U.S.A.* **1992**, *89*, 6653−6657.

(11) Umemoto, U.; Sarma, M. H.; Gupta, G.; Luo, J.; Sarma, R. H. *J. Am. Chem. Soc.* **1990**, *112*, 4539−4545.

(12) Pilch, D. S.; Breslauer, K. J. *Proc. Natl. Acad. Sci. U.S.A.* **1994**, *91*, 9332−9336.

(13) Pilch, D. S.; Kirolos, M. A.; Breslauer, K. J. *Biochemistry* **1995**, *34*, 16107−16124.

(14) (a) Scaria, P. V.; Shafer, R. H. *J. Biol. Chem.* **1991**, *266*, 5417−5423. (b) Tuite, E.; Nordén, B. *Bioorg. Med. Chem.* **1995**, *3*, 701−711.

(15) (a) Lee, J. S.; Latimer, L. J. P.; Hampel, K. J. *Biochemistry* **1993**, *32*, 5591−5597. (b) Latimer, L. J. P.; Payton, N.; Forsyth, G.; Lee, J. S. *Biochem. Cell Biol.* **1995**, *73*, 11−18.

(16) (a) Mergny, J. L.; Duval-Valentin, G.; Nguyen, C. H.; Perrouault, L.; Faucon, B.; Rougée, M.; Montenay-Garestier, T.; Bisagni, E.; Hélène, C. *Science* **1992**, *256*, 1681−1684. (b) Pilch, D. S.; Martin, M-T.; Nguyen, C. H.; Sun, J-S.; Bisagni, E.; Garestier, T.; Hélène, C. *J. Am. Chem. Soc.* **1993**, *115*, 9942−9951. (c) Pilch, D. S.; Waring, M. J.; Sun, J-S.; Rougée, M.; Nguyen, C. H.; Bisagni, E.; Garestier, T.; Hélène, C. *J. Mol. Biol.* **1993**, *232*, 926−946.

(17) (a) Wilson, W. D.; Tanious, F. A.; Mizan, S.; Yao, S.; Kiselyov, A. S.; Zon, G.; Strekowski, L. *Biochemistry* **1993**, *32*, 10614−10621. (b) Cassidy, S. A.; Strekowski, L.; Wilson, W. D.; Fox, K. R. *Biochemistry* **1994**, *33*, 15338−15347.

(18) (a) Collier, D. A.; Neidle, S. *J. Med. Chem.* **1988**, *31*, 847−857. (b) Agbandje, M.; Jenkins, T. C.; McKenna, R.; Reszka, A. P.; Neidle, S. *J. Med. Chem.* **1992**, *35*, 1418−1428.

(19) Tanious, F. A.; Jenkins, T. C.; Neidle, S.; Wilson, W. D. *Biochemistry* **1992**, *31*, 11632−11640.

(20) Neidle, S.; Jenkins, T. C. *Methods Enzymol.* **1991**, *203*, 433−458.

(21) Fox, K. R.; Polucci, P.; Jenkins, T. C.; Neidle, S. *Proc. Natl. Acad. Sci. U.S.A.* **1995**, *92*, 7887−7891.

ω-aminoalkanamide moieties. Thus, **1** and **2** (see Figure 1) represent the 1,4- and 2,6-difunctionalized geometric isomers, respectively. As a prerequisite to a characterization of the binding processes, the self-association properties of these compounds in aqueous solution are also examined. Thermodynamic data were obtained for the DNA−drug interactions using high-sensitivity isothermal titration calorimetry. The results show marked differences in binding enthalpy for interaction of the two isomers with $dA_n{\cdot}dT_n$ duplexes and $dT_n-dA_n{\cdot}dT_n$ triplexes of a defined length. Conclusions from this study are supported by data obtained from UV melting experiments with poly(dA)·poly(dT) and poly(dA)·poly(dT)$_2$, revealing differential stabilizing properties for each ligand with the homopolymeric DNA duplex and triplex. The binding behaviors of these ligands were further probed using competition dialysis techniques, revealing that the 1,4 compound (**1**) shows preferential duplex binding, whereas the 2,6 isomer (**2**) binds most favorably to triplex DNA and thereby behaves as a selective molecular anchor or stabilant. These conclusions support recent molecular modeling and DNA footprinting studies,[20,21] and the data provide a firm quantitative basis for the contrasting modes and energetics of interaction with higher ordered nucleic acids for this class of ligand.

Experimental Section

Materials. Poly(dA)·poly(dT) and poly(dT) were purchased from Pharmacia Biotech as their sodium salts and used without further purification. The polydeoxynucleotides were dissolved in aqueous CNE buffer (10 mM sodium cacodylate, 300 mM sodium chloride, and 0.1 mM EDTA, pH 6.00 ± 0.01) and dialyzed against this buffer for 48 h prior to use. The dA_{18} and dT_{18} octadecadeoxynucleotides were prepared with an Applied Biosystems 391-EP automated synthesizer using standard phosphoramidite chemistry, purified by HPLC, desalted on a Sephadex G-10 exclusion chromatography column, and finally dialyzed against water. In each case, >99% homogeneity was established using capillary electrophoresis. Concentrations of all DNA solutions were determined by UV spectrophotometry using the following extinction coefficients:[13] poly(dA)·poly(dT), $\epsilon_{260} = 12\,000$ M (base pairs) cm^{-1}; poly(dT), $\epsilon_{265} = 8\,700$ M (nucleotide) cm^{-1}, and $\epsilon_{260} = 146\,400$ and 219 400 M (strands) cm^{-1} for dT_{18} and dA_{18}, respectively. The poly(dA)·poly(dT)$_2$ triplex was formed by mixing equimolar (i.e., base pairs to nucleotides) solutions of the poly(dA)·poly(dT) duplex and the poly(dT) single strand, heating to 95 °C, and annealing by slow cooling during 18 h. The $dA_{18}{\cdot}dT_{18}$ duplex and $dT_{18}-dA_{18}{\cdot}dT_{18}$ triplex were prepared in aqueous CNE buffer, pH 6.0, by mixing solutions of the appropriate single strands in 1:1 and 1:2 molar ratios, respectively, and subsequently annealing as described above. The isomeric 1,4- and 2,6-bis[3-(dimethylamino)propionamido]-anthracene-9,10-diones (**1** and **2**, respectively, in Figure 1) were prepared as their water-soluble acid addition salts using published procedures.[18] Both compounds were homogeneous by HPLC and ^{1}H NMR, and their aqueous solutions were quantitated spectrophotometrically using $\epsilon_{438} = 5\,210$ M^{-1} cm^{-1} for **1** and $\epsilon_{355} = 9\,060$ M^{-1} cm^{-1} for **2**.

Optical Studies of Thermal Denaturation. All UV melting experiments were carried out in aqueous CNE buffer using a Varian-Cary 1E spectrophotometer interfaced to an IBM 486/SX computer for data acquisition, with temperature control achieved using a Peltier heating accessory. Heating runs were typically performed between 35 and 98 °C, at a scan rate of 0.5 °C min^{-1} and with optical monitoring at 260 nm. Fixed poly(dA)·poly(dT) duplex or poly(dA)·poly(dT)$_2$ triplex concentrations [20 μM in either base pairs (bp) or base triplets (bt) in CNE buffer, pH 6.0] were used and all melts were performed in 1-cm pathlength quartz cells. Analyses of melting transitions were carried out using supplied Varian-Cary software.

Ligand Self-Association. UV−visible spectra were recorded at 25 °C for a range of ligand concentrations using a Perkin-Elmer Lambda 2 spectrophotometer interfaced with a PCX 386 computer for data collection. Ligand solutions were prepared using aqueous CNE buffer to give accurate concentrations of 0.25 and 0.69 mM for **1** and **2**, respectively. Appropriate dilutions were used to generate a range of concentrations (≥ 1 μM), and optical absorption spectra were recorded from 200 to 600 nm for each solution. These data were used to derive the apparent molar extinction coefficient (see Results and Analysis).

Isothermal Titration Calorimetry (ITC). All calorimetric titrations were performed using a Microcal MCS high-sensitivity isothermal titration calorimeter (Microcal Inc., Amherst, MA) interfaced to a Gateway 2000 PC (486/DX2-66) for data acquisition and analysis. Data from ITC experiments can be used to determine the equilibrium binding constant (K_b), number of binding sites (n) per duplex or triplex, and the enthalpy change (ΔH_{cal}) associated with the DNA−ligand interactions. Binding isotherms were obtained by selecting the concentration of titrate such that $K_b{\cdot}$[titrate] ≥ 10 in all experiments and, over a series of titrations, the ligand concentration was increased up to a maximum of 1.8 mM. Aqueous CNE buffer, pH 6.0, was used for all calorimetry experiments and the experimental temperature was 25.00 ± 0.01 °C. For a typical titration, serial 15-μL injections of ligand solution (1.8 mM) were added at 400-s intervals to a solution containing either $dA_{18}{\cdot}dT_{18}$ duplex or $dT_{18}-dA_{18}{\cdot}dT_{18}$ triplex (42 μM in bp or bt). Each injection produces a peak which corresponds to the power needed to maintain the sample and reference cells at identical temperatures. These peaks can be integrated and corrected for sample concentration and cell volume to produce the heat output per injection.[22,23] Control experiments were performed to determine the heats of dilution for buffer titrated into DNA, and for ligand titrated into buffer; the net enthalpy for each DNA−ligand interaction was calculated by subtraction of the heats of dilution for the component molecules. Thermodynamic parameters were determined from the corrected binding isotherms by fitting to a model based upon a multiple set of independent binding sites,[24] using a nonlinear least-squares fitting procedure in the Origin software package (supplied by the manufacturer).

Competition Dialysis Experiments. Competition dialysis provides an unequivocal technique to establish the binding preferences of a ligand for a particular DNA. Poly(dA)·poly(dT) duplex and poly(dA)·poly(dT)$_2$ triplex solutions of equal concentration (0.7 mM in bp or bt) were placed in separate dialysis chambers and dialyzed against a common buffered ligand solution. After equilibration, the concentration of free ligand will be identical in each compartment, but a preferential interaction with either DNA will lead to an accumulation of total ligand in the appropriate DNA chamber. Experiments were carried out using Spectropore (MW cutoff = 12−14 000) dialysis tubing and aqueous CNE buffer, pH 6.0. In separate experiments, the concentration of either **1** or **2** was varied from 1 to 8 μM. After equilibration for 48 h at 25 °C, the concentrations of free and total ligand in the chambers were determined by UV−visible spectrophotometry following addition of 0.5% sodium dodecyl sulfate (SDS) to dissociate the DNA−ligand complexes. The data were quantified as described in the Results and Analysis section. Control experiments established that neither compound shows significant binding to the dialysis membrane under the solution conditions used.

Results and Analysis

Thermal Denaturation. Figure 2 shows normalized UV melting curves for poly(dA)·poly(dT) and poly(dA)·poly(dT)$_2$ in the absence and presence of **1** and **2**, revealing that both ligands influence the thermal stabilities of duplex and triplex DNA for this homopolymer sequence. The melting profile of the drug-free or native DNA triplex (Figures 2A and 2C: solid line) is biphasic, with thermal transitions at 54.3 and 77.8 °C in the CNE buffer used. The low-temperature event (T_m1 or Hoogsteen transition) corresponds to dissociation of the poly(dT) third strand from the poly(dA)·poly(dT) duplex (i.e., triplex → duplex + strand melting). In contrast, the event observed

(22) Wiseman, T.; Williston, S.; Brandts, J.; Lin, L. *Anal. Biochem.* **1989**, *179*, 131−137.
(23) Ladbury, J. E. *Structure* **1995**, *3*, 635−639.
(24) Cantor, C. R.; Schimmel, P. R. *Biophysical Chemistry, Part III: The Behavior of Biological Macromolecules*; W. H. Freeman: New York, 1980; Chapter 15.

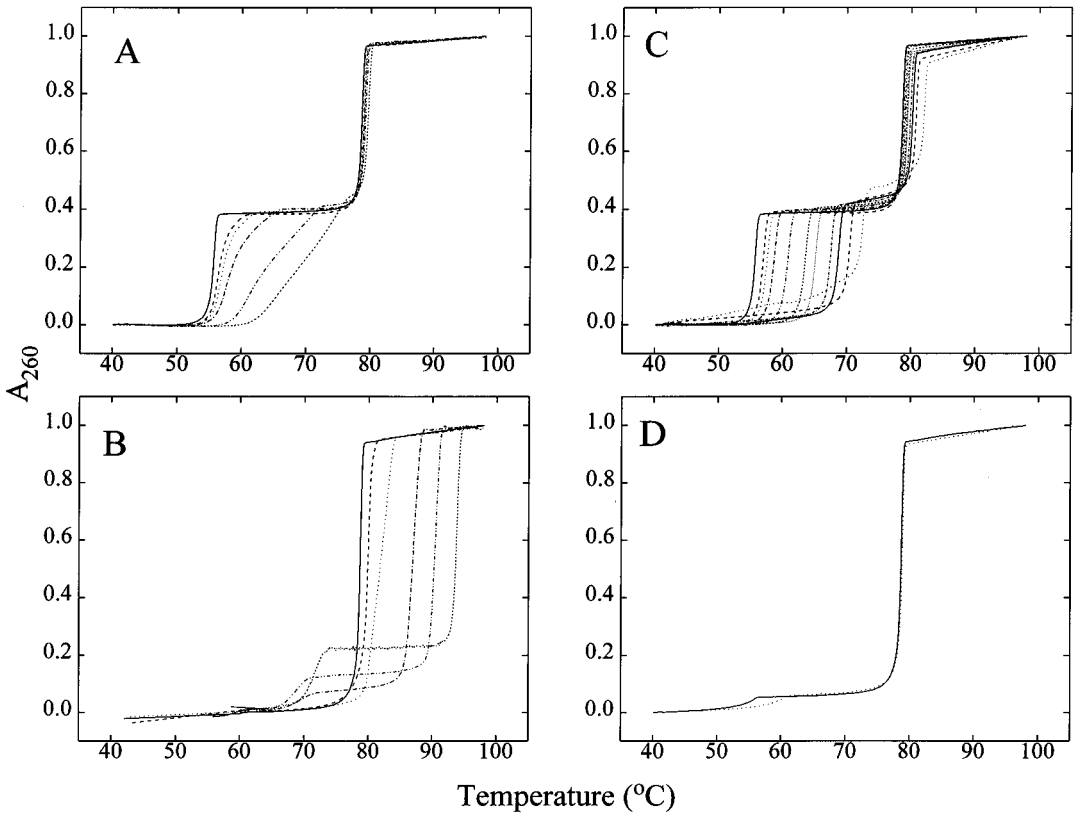

Figure 2. Optical thermal denaturation profiles for the poly(dA)·poly(dT)$_2$ triplex and the poly(dA)·poly(dT) duplex in the absence and presence of **1** (panels A and B, respectively) or **2** (panels C and D, respectively). In panel A, the [**1**]/[triplex (bt)] ratio was restricted to a 0−0.1:1 range as the T_m1 transition was removed at ratios of ≥0.1:1 such that only the T_m2 transition could be detected (see text). In contrast, panel C shows behavior for [**2**]/[triplex] molar ratios in the 0−4:1 range; higher ratios resulted in precipitation of the complex. For the DNA duplex, the [ligand]/[duplex (bp)] ratio was increased from 0−2:1 (**1**, panel B) or 0−0.1:1 (**2**, panel D). All melting curves are normalized to a 0−1 absorbance change for a DNA concentration of 40 μM (bp or bt), using a 1-cm cell and aqueous CNE buffer, pH 6.0.

at higher temperature (T_m2 or Watson−Crick transition) represents helix−coil thermal denaturation of the double-stranded DNA (i.e., duplex → strands melting),[25] as shown in Figures 2B and 2D (solid line) for the poly(dA)·poly(dT) duplex.

Stepwise addition of anthraquinone **2** to the triplex leads to a marked increase of T_m1 but only a modest effect upon T_m2 (Figure 2C). Figure 3B (inset) summarizes the differential T_m effects relative to the native DNA triplex and duplex, indicating induced ΔT_m1 and ΔT_m2 values of 15.1 and 3.4 °C, respectively, at a [**2**]/[triplex (bt)] molar ratio of 2:1. Figure 2D shows the effect of **2** upon the melting of poly(dA)·poly(dT) at a [ligand]/[duplex (bp)] ratio of 0.1:1, confirming a negligible effect upon T_m2 compared to the free DNA duplex. Interestingly, a weak triplex transition detected at 54 °C under these conditions is moved dramatically (∼6 °C) upon addition of **2** even at this low level of added ligand.

Figures 2 and 3B provide clear evidence that **2** has a higher binding affinity for triplex compared to duplex DNA and hence for preferential thermal stabilization of the triple-helical form, with retention of biphasic behavior for [**2**]/[triplex] molar ratios in the 0−1:1 range. However, the melting profiles do not remain biphasic for [ligand]/[triplex] ratios in the 1−4:1 range, and such polyphasic behavior may reflect dissociative ligand redistribution during the melting processes. Thus, for example, strand separation from one portion of the triplex would lead to a release of bound ligand from that site for subsequent binding to a more intact helical segment, thereby increasing the local binding density and thermal stability of that region. This type of melting behavior is consistent with the DNA binding model proposed by McGhee for helix-stabilizing ligands.[26]

Figures 2B and 3A (inset) show data for the interaction of **1** with the poly(dA)·poly(dT) duplex. In the absence of ligand the melting process is clearly monophasic. Upon addition of ligand there is a stabilizing effect of a similar magnitude to that seen for binding of **2** to the triplex, with a ΔT_m of 15.4 °C (i.e., upon T_m2) determined at a [**1**]/[duplex (bp)] ratio of 2:1 which effects saturation of the DNA host. An interesting feature of the melting is the appearance of biphasic behavior at [**1**]/[duplex] ratios >0.5:1. This may be due to either a redistribution of ligand molecules during the melting transition, as discussed above, or secondary binding modes at high [ligand]/[DNA] ratios (e.g., outside-edge association[27] of dicationic ligand to the phosphodiester backbone of the duplex). Figure 2A reveals the effect of **1** upon the melting of the poly(dA)·poly(dT)$_2$ triplex, showing that this ligand induces (i) significant broadening of the Hoogsteen T_m1 transition at very low [ligand]/[DNA] molar ratios and (ii) a complete removal of this transition at ratios ≥0.1:1. Such effects are clearly evident from the derivative plot shown in Figure 3A. This behavior is consistent with a ligand-induced destabilization of this triplex by **1**, leading to an overall disruption of the triple-helical structure. In

(25) (a) Kibler-Herzog, L.; Kell, B.; Zon, G.; Shinozuka, K.; Mizan, S.; Wilson, W. D. *Nucleic Acids Res.* **1990**, *18*, 3545−3555. (b) Pilch, D. S.; Brousseau, R.; Shafer, R. H. *Nucleic Acids Res.* **1990**, *18*, 5743−5750. (c) Wilson, W. D.; Hopkins, H. P.; Mizan, S.; Hamilton, D. D.; Zon, G. *J. Am. Chem. Soc.* **1994**, *116*, 3607−3608.

(26) McGhee, J. D. *Biopolymers* **1976**, *15*, 1345−1375.

(27) (a) Wilson, W. D.; Jones, R. L. In *Intercalation Chemistry*; Whittingham, M. S., Jacobson, A. J., Eds.; Academic Press: New York, 1982; Chapter 14. (b) Wilson, W. D. In *Nucleic Acids in Chemistry and Biology*; Blackburn, G. M., Gait, M. J., Eds.; IRL Press: Oxford, U. K., 1992; pp 295−336.

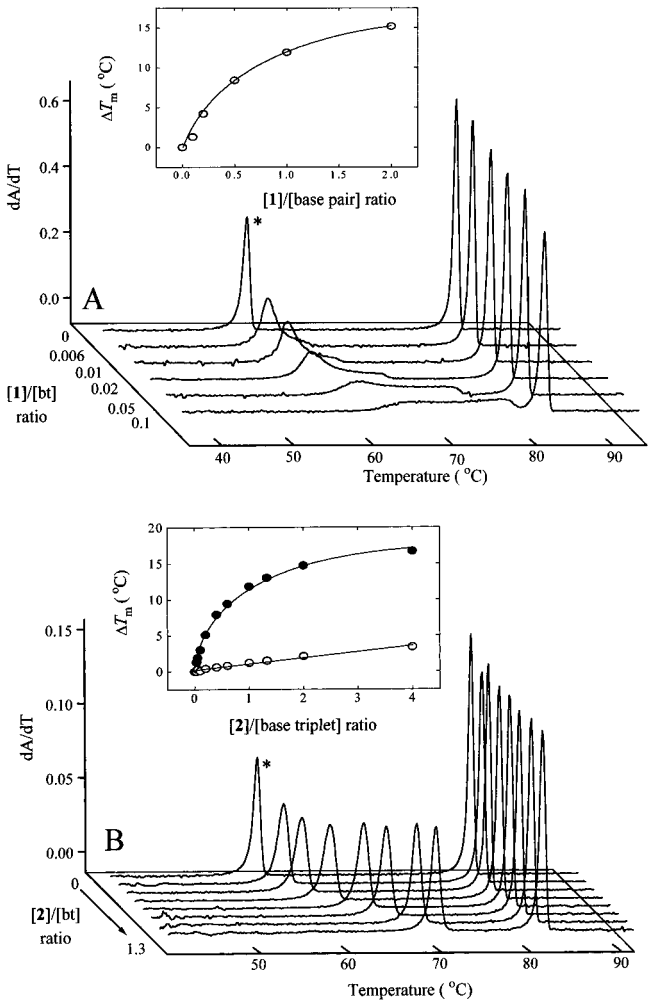

Figure 3. Binding-induced changes in T_m for poly(dA)·poly(dT) and poly(dA)·poly(dT)$_2$ with respect to the drug-free DNA as a function of [ligand]/[DNA] molar ratio. (A) First derivative dA_{260}/dT plot of the optical data in Figure 2A showing the disruptive effect upon the triplex T_m1 transition induced by ligand **1**, compared to the stabilizing effect upon the duplex T_m2 transition. (B) Derivative plot of the data in Figure 2C, indicating strong thermal stabilization of the triplex by ligand **2**, with no significant broadening of the T_m1 transition. In each case the asterisk represents the drug-free DNA control. The inset panels show the differential effects of each ligand upon the low-temperature T_m1 (●: triplex → duplex + single strand) and high-temperature T_m2 (○: duplex → single strands) events, respectively. No triplex stabilization was detectable at [**1**]:[triplex] molar ratios of ≥0.1:1 (see Figure 2).

contrast, no such broadening is observed (cf. Figure 3B) for the isomeric **2** ligand.

Both Ligands Exhibit Self-Association. Interpretation of the DNA−ligand binding data requires evaluation of the ligand self-association behavior to avoid possible complication. The aggregation properties of each ligand were thus examined in aqueous solution using optical absorption spectroscopy to assess any concentration-dependent behavior. Figure 4 shows that the apparent molar extinction coefficient ϵ_{app} determined for **2** is effectively constant for ligand concentrations in the 30−550 μM range, but diminishes gradually at [ligand] <30 μM. In the simplest case if we assume a reversible dimerization model for a monomeric ligand molecule L, then:

$$2L \overset{K_2}{\longleftrightarrow} L_2 \qquad K_2 = [L_2]/[L]^2 \qquad (1)$$

Schwartz et al.[28] have shown that the following relationship

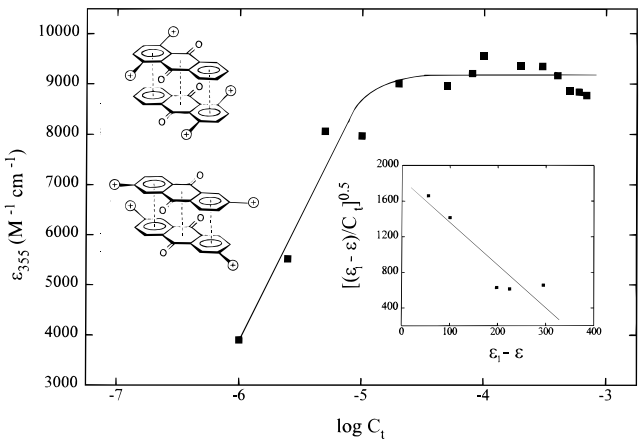

Figure 4. Concentration-dependent variation of the molar extinction coefficient for free ligand **2** determined at 355 nm. Absorbance spectra were measured in aqueous CNE buffer for a range of concentrations using either a 0.1- or 1-cm pathlength cell. The sigmoidal relationship is characteristic of ligand self-association.

holds for a dimer model:

$$\left[\frac{\epsilon_1 - \epsilon_{app}}{C_t}\right]^{1/2} = \left(\frac{2K_2}{\Delta\epsilon}\right)^{1/2} [\Delta\epsilon - (\epsilon_1 - \epsilon_{app})] \qquad (2)$$

where ϵ_{app} is the apparent extinction coefficient, ϵ_1 is the extinction coefficient of the monomer, $\Delta\epsilon$ is the difference in extinction coefficient for the monomer and dimer species, K_2 is the equilibrium dimerization constant, and C_t is the total drug concentration. In this case, eq 2 can be used to determine K_2 since a plot of $[(\epsilon_1 - \epsilon_{app})/C_t]^{1/2}$ against $(\epsilon_1 - \epsilon_{app})$ will give an x-axis intercept of $\Delta\epsilon$ and a linear slope of $(2K_2/\Delta\epsilon)^{1/2}$.

Figure 4 (inset) shows the analysis obtained for anthraquinone **2**, indicating a K_2 value of (3.2 ± 0.1) × 10^3 M^{-1} at 25 °C (r = 0.96) for dimerization of this compound. Analogous behavior was observed for the 1,4 isomer leading to a K_2 value of (2.9 ± 0.2) × 10^3 M^{-1} for **1** at 20 °C (r = 0.89; data not shown). The satisfactory linear fits obtained for each molecule indicate that the dimer model is appropriate and that higher-order polymeric structures or aggregates are not involved.[28] Molecular modeling studies (not shown) indicate that dimerization can result in plausible structures with maximum $\pi-\pi$ overlap of each neighboring monomer subunit (e.g., Figure 4); higher multimers are unfavorable due to stacking requirements for charge and/or steric clash avoidance. On this basis, we interpret our data in terms of a simple dimerization model for both **1** and **2** isomers. NMR studies have similarly shown that BePI self-associates in aqueous solution, although it was not possible to distinguish between dimerization and formation of *n*-mer multimers.[16b]

Isothermal Titration Calorimetry (ITC). The binding enthalpies for interaction of **1** and **2** with triplex and duplex DNA were determined directly using high-sensitivity ITC. Figures 5A and 5B show primary data for titration addition of **2** to the dA$_{18}$·dT$_{18}$ duplex and dT$_{18}$−dA$_{18}$·dT$_{18}$ triplex, respectively. Integration, with respect to time, of the heats produced per injection (peaks in upper panels), with an appropriate correction to a per mole basis, gives the corresponding binding isotherm (lower panels). These data must be corrected for the dilution heats associated with the addition of (i) buffer into DNA and (ii) drug into buffer. In the first control experiments, the heat of dilution for the buffer into DNA was shown to be constant and negligible. In contrast, titration of the drug into

(28) Schwartz, G.; Klose, S.; Balthasan, W. *Eur. J. Biochem.* **1970**, *12*, 454−460.

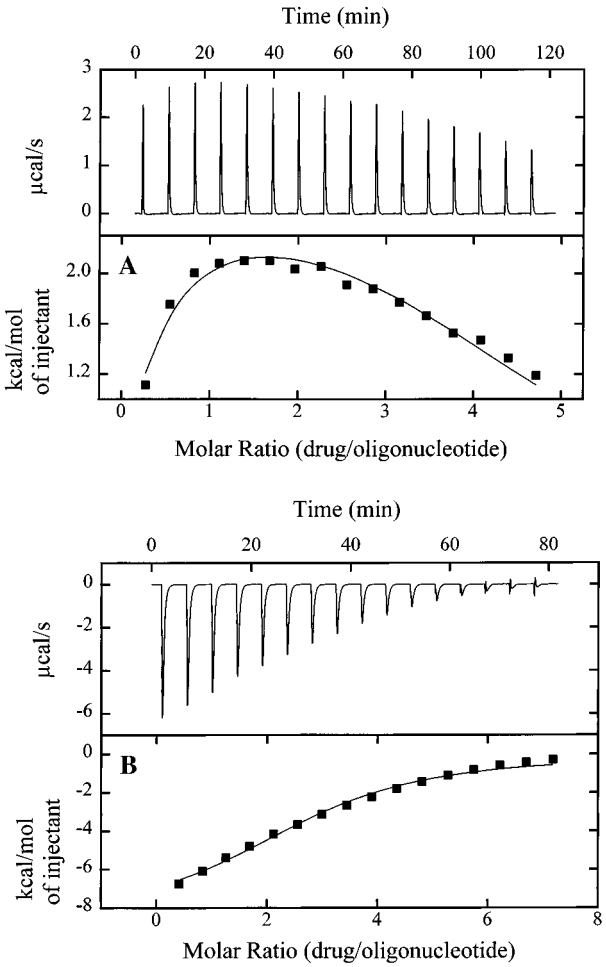

Figure 5. (A) Raw calorimetric data for the titration of $dA_{18}{\cdot}dT_{18}$ duplex with ligand **2** determined at 25 °C, showing endothermic binding. The top panel represents the power output associated with each 15-μL injection of titrant as a function of time. Integration of these peaks (using standard software supplied by Microcal Inc.) yields the heat produced per injection as a function of [ligand]/[duplex] molar ratio (bottom panel). The initial DNA concentration in the cell was 80 μM (bp) and the ligand concentration was 1.8 mM. (B) ITC data for the interaction of **2** with the $dT_{18}-dA_{18}{\cdot}dT_{18}$ triplex, generated in an identical manner. In contrast to the duplex binding, interaction of **2** with the triplex is exothermic. The initial concentration of DNA in the sample cell was 50 μM (bt) and the concentration of ligand titrant was 1.8 mM.

aqueous buffer was found to be significant. The titration profile obtained (Figure 6A) is typical for the heats produced by a ligand undergoing dissociation[29] and corroborates our spectrophotometric observations of drug self-association leading to a dimeric species (see above).

The enthalpy change (ΔH_{obs}) upon titration of oligonucleotide with concentrated drug solution is given by:

$$\Delta H_{obs} = \Delta H_{dissoc} + \Delta H_{binding} \qquad (3)$$

where ΔH_{dissoc} represents the enthalpy for dissociation of the dimer to the DNA-binding species,[29] but was not here determined as a separate parameter. The heats of dilution, which incorporate ΔH_{dissoc}, can be subtracted from the raw calorimetric data in the usual way,[22] as shown in Figure 6B. This treatment has no significant influence upon the thermodynamic measurements for the equilibrium binding processes in the present study since, for the K_2 values determined for ligand dimerization and

(29) Roche, C. J.; Thomson, J. A.; Crothers, D. M. *Biochemistry* **1994**, *33*, 926−935.

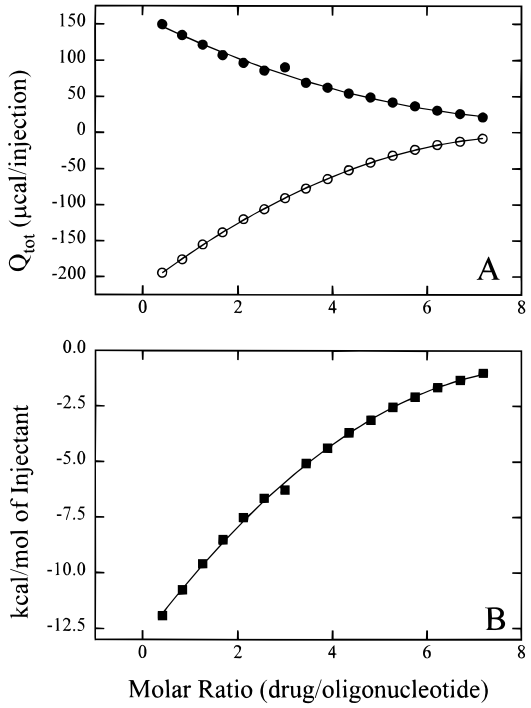

Figure 6. (A) Comparison of the heats of dilution obtained from titration of **2** into aqueous CNE buffer (●) with the values determined from addition to the $dT_{18}-dA_{18}{\cdot}dT_{18}$ triplex (○). The titration curve for the dilution experiment shows decreased heat output with increased ligand concentration in the cell, indicating self-association. Simple subtraction to obtain corrected binding enthalpies is thus not possible (see text). (B) Corrected binding isotherm for interaction of **2** with the 18-mer triplex, obtained after subtraction of the heats of dilution determined for the ligand and DNA reactants.

a given ligand titrant concentration (e.g., 1.8 mM), only a negligible concentration of dimeric species (~3% of total ligand) will remain in the cell at the end of a titration. On this basis, it was not necessary to determine the heats of infinite dilution for each ligand. For significantly larger K_2 values, the heats of dilution obtained in the absence and presence of DNA would differ, such that the heat for ligand dilution into buffer cannot be subtracted from the heats produced in a binding experiment.[29]

Application of the multiple independent binding sites model leads to optimal fitting for the ITC data for the interactions of **1** and **2** with host oligonucleotide duplex and triplex structures. Using this model, the binding enthalpy ($\Delta H°$), equilibrium binding constant (K_b), and number of binding sites (n) can be determined (Table 1); the remaining thermodynamic parameters can be calculated using the standard relationships:

$$\Delta G° = -RT \ln K_b \qquad \Delta S° = (\Delta H° - \Delta G°)/T$$

Table 1 shows that the DNA−ligand interactions leading to stabilization of the 18-mer duplex or triplex are exothermic. Thus, overall binding of **1** to the duplex is weakly enthalpic, whereas the **1**−triplex interaction has both a large enthalpic component and a significant entropic term, suggesting that this ligand entropically destabilizes the triple-stranded structure. In contrast, the enthalpy for **2**−duplex binding is compensated by the entropy component for the interaction whereas the **2**−triplex interaction is enthalpically driven. Similar binding stoichiometries are obtained for the DNA structures with each ligand, indicating mean binding site sizes that span 3.6−4.5 base pairs of the duplex or 3.6 base triplets of the triple-stranded structure.

In accord with our UV melting studies, **1** binds more tightly to the duplex compared to the triplex (3-fold preference),

Table 1. Thermodynamic Parameters[a] for Ligand Binding to Duplex and Triplex DNA

DNA	compd	$\Delta H°$ (kcal mol^{-1})	$\Delta G°$ (kcal mol^{-1})	$T\cdot\Delta S°$ (kcal mol^{-1})	K_b ($\times 10^4$ M^{-1})	site size (bp/bt)	n^b	ΔT_m[c] (°C)
$dA_{18}\cdot dT_{18}$	**1**	−2.7	−6.7	+4.0	11	3.6	5	15.4
	2	+0.8	−5.8	+6.6	1.8	4.5	4	3.4
$dT_{18}-dA_{18}\cdot dT_{18}$	**1**	−28.3	−6.3	−22.0	3.5	3.6	5	—[d]
	2	−7.9	−7.3	−0.6	22	3.6	5	15.1

[a] Calorimetric data refer to an experimental temperature of 298 K (25 °C); $\Delta H°$, $\Delta G°$, $T\cdot\Delta S°$ and K_b are expressed in moles of either duplex or triplex. Estimated errors are as follows: $\Delta H°$ (±0.3 kcal mol^{-1}), $\Delta G°$ (±0.6 kcal mol^{-1}), $T\cdot\Delta S°$ (±0.4 kcal mol^{-1}), ΔT_m (±0.1 °C), and K_b (±0.6 × 10^4 M^{-1}). [b] Number of distinct ligand binding sites (i.e., 18/site size) determined for the DNA duplex or triplex (see text). [c] Optical thermal denaturation data refer to a [ligand]/[DNA (bp or bt)] molar ratio of 2:1. [d] No thermal stablilization could be detected at [ligand]/[DNA] ratios of ≥0.1:1 due to disruption of the DNA triplex (see text).

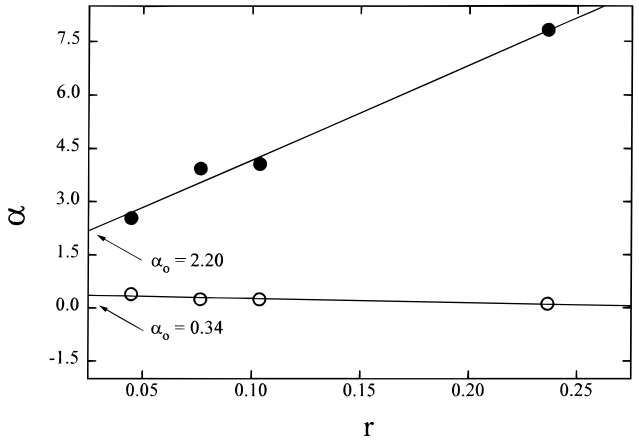

Figure 7. Competition dialysis data from experiments designed to assess the binding preferences of **1** (○) or **2** (●) with the poly(dA)·poly(dT) duplex and the poly(dA)·poly(dT)$_2$ triplex in aqueous CNE buffer, pH 6.0. The least-squares fitted lines yield intercept α_0 (i.e., triplex/duplex) values of 0.34 and 2.20, indicating favored duplex binding for **1** and triplex binding for **2**, respectively (see text).

whereas **2** binds preferentially to the DNA triplex by a ∼12-fold factor. Further, comparison of K_b values reveals a 6-fold duplex-binding preference for the isomer **1** compared to **2**, and a contrasting opposite 6-fold triplex-binding preference for **2** relative to **1**. These distinctions highlight the differential binding of the two isomeric ligands and agree with experimental observations reported for such isomers,[21] molecular modeling,[20,21] and competitive fluorescence displacement studies using duplex DNA (Jenkins, Polucci, and Neidle, unpublished data).

Preferential DNA−Ligand Binding. The results from the UV melting studies and calorimetric experiments indicate that **2** binds preferentially to triplex DNA whereas the 1,4 isomer **1** favors binding to duplex-form DNA. Competition dialysis experiments were performed to unambiguously establish the DNA duplex/triplex binding preferences for each isomeric ligand. Figure 7 shows the results obtained using identical concentrations of poly(dA)·poly(dT) and poly(dA)·poly(dT)$_2$ following dialysis against a common solution of ligand. At equilibrium (48 h), the concentration of unbound ligand will be identical in all three compartments; however, preferential binding to either duplex or triplex will result in accumulation of bound ligand in the dialysis chamber containing the favored DNA. The data may be quantified by plotting the α parameter against the molar binding ratio r:

$$r = [C_b]/[\mathrm{DNA}]_{total} \quad (4)$$

$$\alpha = r_{triplex}/r_{duplex} \quad (5)$$

where C_b is the concentration of bound drug, $[\mathrm{DNA}]_{total}$ is the total concentration of either triplex or duplex, and r_{duplex} and $r_{triplex}$ are the corresponding molar binding ratios. The intercept value of α when $r = 0$ (i.e., α_0) provides an indicator of the favored DNA for complexation by each ligand.[30,31] Figure 7 confirms that **1** accumulates in the chamber containing duplex DNA ($\alpha_0 = 0.34$), whereas **2** accumulates in the triplex DNA compartment ($\alpha_0 = 2.2$). The binding specificities of the two geometric isomers are thus markedly different.

It should be noted that, at the high ionic strength (300 mM) used in these experiments, the possible influences of Donnan-type equilibria upon ligand distribution due to polyelectrolyte or counterion behaviors associated with the two DNA structures are probably insignificant.

Discussion

The principal conclusions that can be drawn from the present studies are as follows: (i) both ligands show self-association in aqueous solution; (ii) the two ligands are able to discriminate between triplex and duplex DNA and thereby show differential binding; (iii) the favored interaction of **1** to double-stranded DNA and binding of **2** to triplex DNA is exothermic and enthalpically driven in each case; (iv) the 1,4 isomer **1** behaves as a triplex-disrupting ligand; and (v) the binding site sizes for the isomeric ligands with each DNA structure are similar. However, there is spectrophotometric evidence for a secondary binding mode in the interaction of **1** with duplex DNA.

Spectroscopic Evidence for the Binding Preferences. Measurements of optical absorbance of a DNA solution as a function of temperature provide a convenient method to establish the denaturation or melting temperature (T_m) of a particular DNA sample. Increases in T_m upon addition of a candidate ligand are frequently used as an indicator of DNA−ligand binding and the extent of induced thermal stabilization can often be compared for families of drugs and DNA sequences. Under certain ideal conditions, it is possible to derive quantitative information about the interaction(s) from the thermal denaturation data. Thus, for example, McGhee has shown[26] that T_m measurements for free and ligand-saturated DNA can be used to determine the enthalpy of melting for the complex, the exclusion behavior of the bound molecule and, importantly, the equilibrium binding constant K_b at $T = T_m$.

We have not attempted to analyze the results from our UV denaturation studies (Figure 2) due to the biphasic nature of the thermal transitions obtained with the DNA triplex and the polyphasic and/or aggregation behavior encountered at high [ligand]/[DNA] molar ratios that approach saturation levels. Further, isothermal titration calorimetry (ITC) provides an inherently superior technique to probe the DNA−ligand binding processes and obtain thermodynamic parameters directly thus avoiding the high temperatures necessarily associated with thermal denaturation experiments. Nevertheless, Figures 2 and 3 clearly emphasize that the two isomers under examination

(30) Chaires, J. B. In *Advances In DNA Specific Agents*; Hurley, L. H., Ed.; JAI Press Inc.: Greenwich, CT, 1992; Vol. 1, pp 3−24.
(31) Müller, W.; Crothers, D. M. *Eur. J. Biochem.* **1975**, *54*, 267−277.

have different affinities for triplex and duplex DNA. Thus, **2** effects marked thermal stabilization of the poly(dA)·poly(dT)$_2$ triplex whereas **1** induces disruption of this triplex, leading to favored stabilization of the released poly(dA)·poly(dT) homopolymer duplex.

Isothermal Titration Calorimetry Gives Nonsigmoidal Binding Isotherms. ITC can be used to measure the heat of binding during addition of titrant for any ligand−macromolecule interaction with a non-zero binding enthalpy. A sigmoidal binding isotherm will result if there is either a single binding site per macromolecule or a number of equivalent or degenerate sites, even where such sites are not necessarily independent. In the case of multiple non-identical sites with different intrinsic binding affinities, the resulting isotherm will be a composite and non-sigmoidal.

The data shown in Figure 5 indicate that not all the potential binding sites on the oligonucleotide structures are identical. Binding sites associated with the internal portion of the 18-mer duplex or triplex would be expected to differ significantly from those nearer the strand termini, particularly where the bound intercalant also occupies a segment of the helical groove(s), and neighbor exclusion effects will be significant. Similarly, alterations in binding affinity may result if association with a ligand induces structural changes in the global DNA triplex or duplex that influence binding of a subsequent ligand molecule. Such effects would become more manifest at higher [ligand]/[DNA] molar ratios.

Only limited structural information is presently available for DNA triplexes.[2,32] However, by analogy with duplex DNA, triplex intercalation would be predicted to require a local structural change of the host involving axial displacement of consecutive triplet base planes in order to accommodate the planar intercalant. Such a process, achieved through conformational changes (e.g., concerted rotation of all three phosphodiester backbones), will result in an overall helical lengthening for the triplex. Binding-induced structural changes of this nature may affect the binding of subsequent ligands since an increasingly drug-bound duplex or triplex host would be expected to become more markedly dissimilar to the drug-free DNA.

Binding Affinities and Stoichiometry. ITC provides the only means to directly determine the molar calorimetric binding enthalpy ($\Delta H°$), which can then be used to determine the equilibrium binding constant (K_b) for a bimolecular DNA−ligand interaction, since other methods invoke the use of the van't Hoff relationship. The trends observed in our thermal melting studies are mirrored in the determined K_b values (Table 1), with the rank order for duplex binding given by **1** > **2** whereas the reverse **2** > **1** ranking is found for binding to the 18-mer triplex. The K_b values of $(1-2) \times 10^5$ M^{-1} for the favored **1**−duplex and **2**−triplex interactions were determined under high-salt or near-physiological (300 mM NaCl) aqueous conditions, showing that binding is moderately tight. These binding constants compare favorably with values established from independent equilibrium and kinetic spectrophotometric studies with oligonucleotide duplexes.[18,19,33]

The stoichiometries for ligand binding with the 18-mer oligonucleotides used in the present experiments indicate average DNA binding sites that span 3.6−4.4 bp (duplex) or 3.6 bt (triplex). It is notable that such sites are identical with the duplex binding site size obtained for a range of 2,6-disubstituted anthraquinones from UV titration studies assuming a neighbor exclusion binding model,[18b] suggesting common intercalative modes of interaction with the double- and triple-stranded DNA structures. Further, the lengths of the spanned or occluded bases are entirely consistent with those predicted from molecular models for intercalative DNA binding,[18,20,21] where the protonated side chains are positioned within the grooves of the host duplex or triplex. The interatomic $N^+ \cdots N^+$ separations determined for **1** (15.0 Å) and **2** (19.8 Å) in their low-energy fully extended structures would be predicted to afford considerably longer binding sites if exclusive groove or outside-edge[27] (i.e., electrostatic) modes of DNA interaction were involved. The similarity found for the present duplex and triplex thus provides indirect evidence of a common intercalative mode for binding with these hybrid ligands.

Calorimetric Enthalpies for DNA Binding with the Isomeric Ligands. The binding enthalpies (Table 1) determined for the **1**−dA$_{18}$·dT$_{18}$ and **2**−dT$_{18}$−dA$_{18}$·dT$_{18}$ interactions (i.e., −2.7 kcal mol (bp)$^{-1}$ and −7.9 kcal mol (bt)$^{-1}$, respectively) are typical for intercalative ligand binding to DNA. Only limited thermodynamic data are presently available for intercalative triplex binding with other ligands, hence comparisons can be made only for analogous binding with duplex DNA (e.g., $\Delta H = -8.8$ kcal mol (bp)$^{-1}$ for binding of ethidium bromide[34] to the calf thymus DNA duplex). The small entropy term for the **2**−triplex interaction indicates that binding to the DNA is *enthalpically driven*. The converse is true for interaction of **2** with the 18-mer DNA duplex, where binding is largely *entropically driven*.

Most established DNA intercalants do not bind well to poly(dA)·poly(dT) or the dA$_n$·dT$_n$ oligomer due to the unusual structural properties associated with these homopolymeric duplexes.[35,36] For example, Chaires has reported[36] that daunomycin binds ∼10-fold less tightly to this sequence than to alternating copolymers. The low binding affinities are also usually accompanied by endothermic binding enthalpies. On this basis, it is likely that the thermodynamic parameters we have obtained for interaction of **1** and **2** with dA$_{18}$·dT$_{18}$ may not be representative for binding to more regular B-type DNA duplexes. Nevertheless, our use of homopolymer DNA sequences is justified as the major aim of the present study is to compare ligand stabilization for a Pu·Py duplex and the derived Py−Pu·Py triplex.

Molecular Interpretation of Thermodynamic Data. Examination of Table 1 allows an assessment of the molecular interaction(s) that stabilize the DNA−ligand complexes. Intermolecular hydrogen-bonded and van der Waals interactions are generally characterized by negative binding enthalpy (ΔH) and entropy (ΔS) terms, whereas electrostatic interactions are usually manifest as small ΔH and positive ΔS components. In contrast, hydrophobic interactions are characterized by positive ΔH and ΔS terms, together with negative heat capacity changes.[37]

Intercalation involves the positioning of a planar aromatic moiety between the stacked base pair or triplet planes of the DNA duplex and triplex, such that the essentially hydrophobic chromophore achieves favorable interactions within the interplane cavity. Hydrophilic and/or nonplanar residues associated with the intercalant will resist insertion into the hydrophobic

(32) (a) Betts, L.; Josey, J. A.; Veal, J. M.; Jordan, S. R. *Science* **1995**, *270*, 1838−1841. (b) Kiran, M. R.; Bansal, M. *J. Biomol. Struct. Dyn.* **1995**, *13*, 493−505.

(33) Armitage, B.; Yu, C.; Devadoss, C.; Schuster, G. B. *J. Am. Chem. Soc.* **1994**, *116*, 9847−9859.

(34) Hopkins, H. P.; Fumero, J.; Wilson, W. D. *Biopolymers* **1987**, *29*, 445−459.

(35) Fox, K. R. *Nucleic Acids Res.* **1990**, *18*, 5387−5391.

(36) (a) Chaires, J. B. *Biochemistry* **1983**, *22*, 4204−4211. (b) Herrera, J. E.; Chaires, J. B. *Biochemistry* **1989**, *28*, 1993−2000.

(37) (a) Kauzmann, W. *Adv. Protein Chem.* **1959**, *14*, 1−63. (b) Eftink, M. R.; Biltonen, R. L. In *Biological Microcalorimetry*; Academic Press Inc.: New York, 1980; pp 343−412.

regions of the oligonucleotide and instead make favorable interactions in the available groove conduits. The thermodynamic parameters (Table 1) and the UV melting analyses provide an indication of differential binding properties of the two anthraquinones. Favorable contributions to free energy are derived from exothermic events such as the formation of noncovalent bonds. In addition, ΔG can be improved by favorable positive entropic effects resulting in a net increase in the degrees of freedom of the system such as the liberation of water molecules from a hydrophobic surface into the bulk medium (i.e., solvent displacement[38]). The duplex and triplex binding of **1** results from significant entropic component terms, whereas the enthalpic contributions to the binding of **2** with either DNA are countered by a unfavorable entropic penalty. As such, the isomeric ligands clearly bind in a contrasting fashion.

Taking the case for the duplex−ligand interaction and assuming that the binding contributions from the two anthraquinone molecular fragments are constant and favorable, then the enthalpic contribution to free energy for the binding of **1** suggests that the functionalized side chains achieve a secondary interaction with the duplex whereas those of the 2,6-disubstituted molecule do not. This observation is supported by the entropic cost for an intimate interaction of the substituents of **1** with the duplex.

The enthalpic terms for binding of each ligand with the DNA triplex indicate that **1** is similarly capable of more energetically favorable nonbonded contacts than **2**, although the large entropic penalty here results in a weaker overall interaction. The effective length of the planar surface of **2** is >11 Å along the long chromophore axis;[20,21] such planarity may be excessive for a duplex intercalation site but may be appropriate to the structural requirements for triplex intercalation. In contrast, the shorter effective chromophore length associated with **1** is likely to be more suitable for intercalation within a DNA duplex rather than triplex site.

Triplex binding of **1** would also be expected to induce significant DNA structural perturbation due to steric effects involving the proximate side chains; such groups would be accommodated within the major groove of a DNA duplex.[18−20] Thus, in effect, both **1** and the third-strand oligonucleotide of the triplex can be envisaged to compete for the duplex major groove, with the net result that the DNA triplex is entropically destabilized. Triplex groove accommodation of **1** would ameliorate such perturbation effects but there is likely to be a loss of favorable base−intercalant stacking. The large negative enthalpy term observed for binding of **1** to the triplex DNA therefore seems anomalous.

Differential displacement of minor groove hydration water from $dA_n{\cdot}dT_n$ duplexes may also be a contributory factor in the binding processes.[38] Competitive groove accommodation of the flexible side chains would probably exact an endothermic penalty although, in certain cases, such energetic costs may be partially offset by external hydration[38b] of the DNA−drug complex. Similarly, triplex-specific hydration may influence the thermodynamics of ligand binding but the possible contributions from such effects are presently unknown.

DNA Structural Preferences of 1,4- and 2,6-AAQ. Competition dialysis techniques provide a direct method to obtain the DNA-binding preferences of a candidate ligand.[30,31] We have used this technique to show that the two isomeric ligands show opposite preferences for the high-order DNA structures. The data unambiguously reveal that **1** binds preferentially to homopolymeric duplex-form Pu·Py DNA, whereas **2** favors binding to the Py−Pu·Py DNA triplex. These experimental conclusions agree with both our thermal denaturation data and calorimetric results.

Summary

Isothermal titration calorimetry and UV spectroscopy have been used to establish complete thermodynamic profiles for the interaction of two isomeric bis(functionalized) anthracene-9,10-diones with homopolymeric duplex and triplex DNA containing $dA_n{\cdot}dT_n$ and $dT_n-dA_n{\cdot}dT_n$ base sequences. The stronger binding of **1** to duplex and **2** to triplex is enthalpically driven and due to electrostatic interactions. The interactions of **1** with triplex (entropically driven) and **2** with duplex (enthalpy/entropy compensated) largely reflect their hydrophobic interaction factors. The data from optical studies of thermal denaturation, competition dialysis, and calorimetric experiments indicate clear binding preferences for these ligands, such that **2** preferentially binds to triplex-form DNA whereas binding of **1** is markedly more favorable with the corresponding duplex. The thermodynamic profiles obtained from these studies provide solid and unambiguous evidence for these contrasting binding behaviors. Such information is valuable for the rational drug design of new triplex stabilants with superior differential DNA triplex/duplex specificity that can be exploited for therapeutic gain in antigene-directed triplex strategies.

Acknowledgment. This research was supported by the Cancer Research Campaign (T.C.J.). We thank Tony Reszka (ICR) for synthesis and exhaustive purification of the oligonucleotides. We are particularly grateful to Professor J. B. Chaires and Dr. J. A. Thomson for helpful discussions.

JA961907T

(38) (a) Marky, L. A.; Kupke, D. W. *Biochemistry* **1989**, *28*, 9982−9988. (b) Nunn, C. M.; Jenkins, T. C.; Neidle, S. *Biochemistry* **1993**, *32*, 13838−13843. (c) Berman, H. M. *Curr. Opin. Struct. Biol.* **1994**, *4*, 345−350.